Role of the sarcin-ricin loop of 23S rRNA in biogenesis of the 50S ribosomal subunit

Sepideh Fakhretaha Aval[1,2], Amal Seffouh[3,4], Kyung-Mee Moon[5], Leonard J. Foster[5], Joaquin Ortega[3,4], and Kurt L. Fredrick[1,2,6,*]

[1]Ohio State Biochemistry Program, The Ohio State University, Columbus, OH 43210, USA.
[2]Center for RNA Biology, The Ohio State University, Columbus, OH 43210, USA.
[3]Department of Anatomy and Cell Biology, McGill University, Montreal, Quebec H3A 0C7, Canada.
[4]Centre for Structural Biology, McGill University, Montreal, Quebec H3G 0B1, Canada.
[5]Department of Biochemistry and Molecular Biology, Michael Smith Laboratories, University of British Columbia, Vancouver, British Columbia, V6T1Z4, Canada.
[6]Department of Microbiology, The Ohio State University, Columbus, OH 43210, USA.

*Corresponding author: Kurt Fredrick (Tel: +1 614 292 6679, Email: fredrick.5@osu.edu)

This supplement contains:

Supplementary Figures S1 to S11

Supplementary Tables S2 to S3

Supplementary References

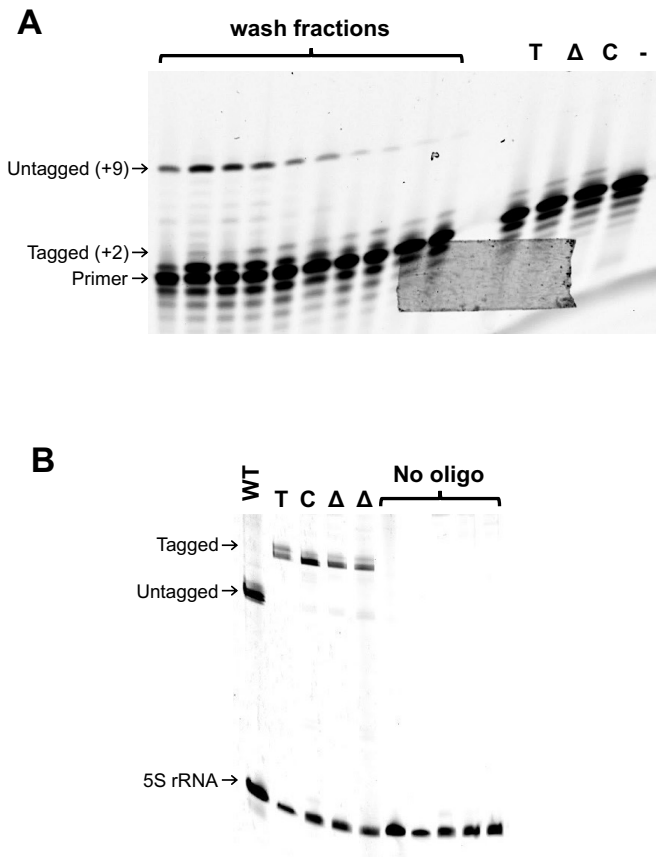

Supplementary Figure S1. ***Evaluation of the purity of aptamer-tagged particles.*** *(A) Examples of poisoned primer extension products used to quantify aptamer-tagged versus untagged 23S rRNA in various samples, as indicated. Lanes on the left correspond to wash fractions from a GSTrap column purification of ΔSRL subunits. Lanes on the right correspond to affinity-purified subunits. As a control, homogeneous aptamer-tagged ribosomes were conventionally purified from the ⊿7 prrn strain KLF2066, which harbors p278MS2 as the only source of rRNA. RNA of these fully tagged (T) ribosomes was analyzed along with RNA of affinity-purified ΔSRL (Δ) and control (C) 50S particles. A reaction without RNA (-) was run in the last lane. Quantification of the T, Δ, and C lanes gave values (% tagged) of 100, 95, and 97, respectively. (B) Example of an RNase H digestion experiment to distinguish tagged versus untagged 23S rRNA in various samples. The lower band corresponds to 5S rRNA. RNA from untagged wild-type (WT) ribosomes and fully tagged (T) KLF2066 ribosomes were used as controls and analyzed alongside RNA from affinity-purified control (C) and ΔSRL (Δ) 50S particles. Two independent preparations of ΔSRL (Δ) particles were analyzed (lanes 4 and 5). Control reactions without DNA oligonucleotide (No oligo; lanes 6-10) were run in parallel. Quantification of the WT, T, C, Δ, and Δ lanes gave values (% tagged) of 0, 100, 99, 97, and 95, respectively.*

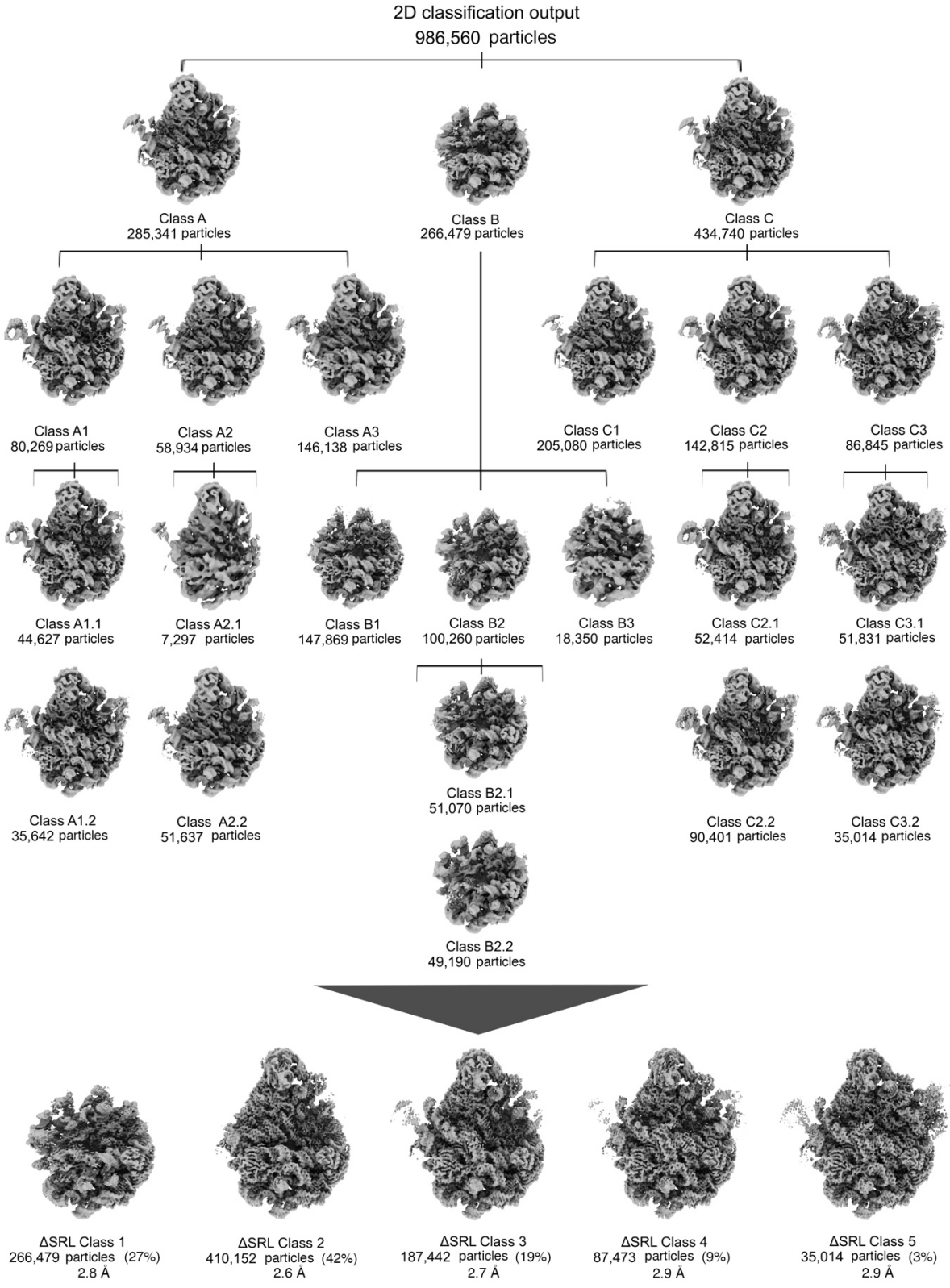
2D classification output
986,560 particles
Class A
285,341 particles
Class B
266,479 particles
Class C
434,740 particles
Class A1
80,269 particles
Class A2
58,934 particles
Class A3
146,138 particles
Class C1
205,080 particles
Class C2
142,815 particles
Class C3
86,845 particles
Class A1.1
44,627 particles
Class A2.1
7,297 particles
Class B1
147,869 particles
Class B2
100,260 particles
Class B3
18,350 particles
Class C2.1
52,414 particles
Class C3.1
51,831 particles
Class A1.2
35,642 particles
Class A2.2
51,637 particles
Class B2.1
51,070 particles
Class C2.2
90,401 particles
Class C3.2
35,014 particles
Class B2.2
49,190 particles
ΔSRL Class 1
266,479 particles (27%)
2.8 Å
ΔSRL Class 2
410,152 particles (42%)
2.6 Å
ΔSRL Class 3
187,442 particles (19%)
2.7 Å
ΔSRL Class 4
87,473 particles (9%)
2.9 Å
ΔSRL Class 5
35,014 particles (3%)
2.9 Å

Supplementary Figure S2. ***3D classification and refinement workflow for the ΔSRL particles isolated from cells.*** *Mutant ΔSRL particles isolated from cells were imaged by cryo-EM, and images were subjected to three layers of 3D classification. For each layer, particles were split into three or two new classes. The resulting subclasses were grouped into five main classes. Particles in these five groups were used to produce the high-resolution cryo-EM maps shown at Figure 3A. The high-resolution cryo-EM maps are shown unsharpened. The number of particles used for the final refinement of each class, the percentage of the total population they represent, and the obtained resolution are indicated.*

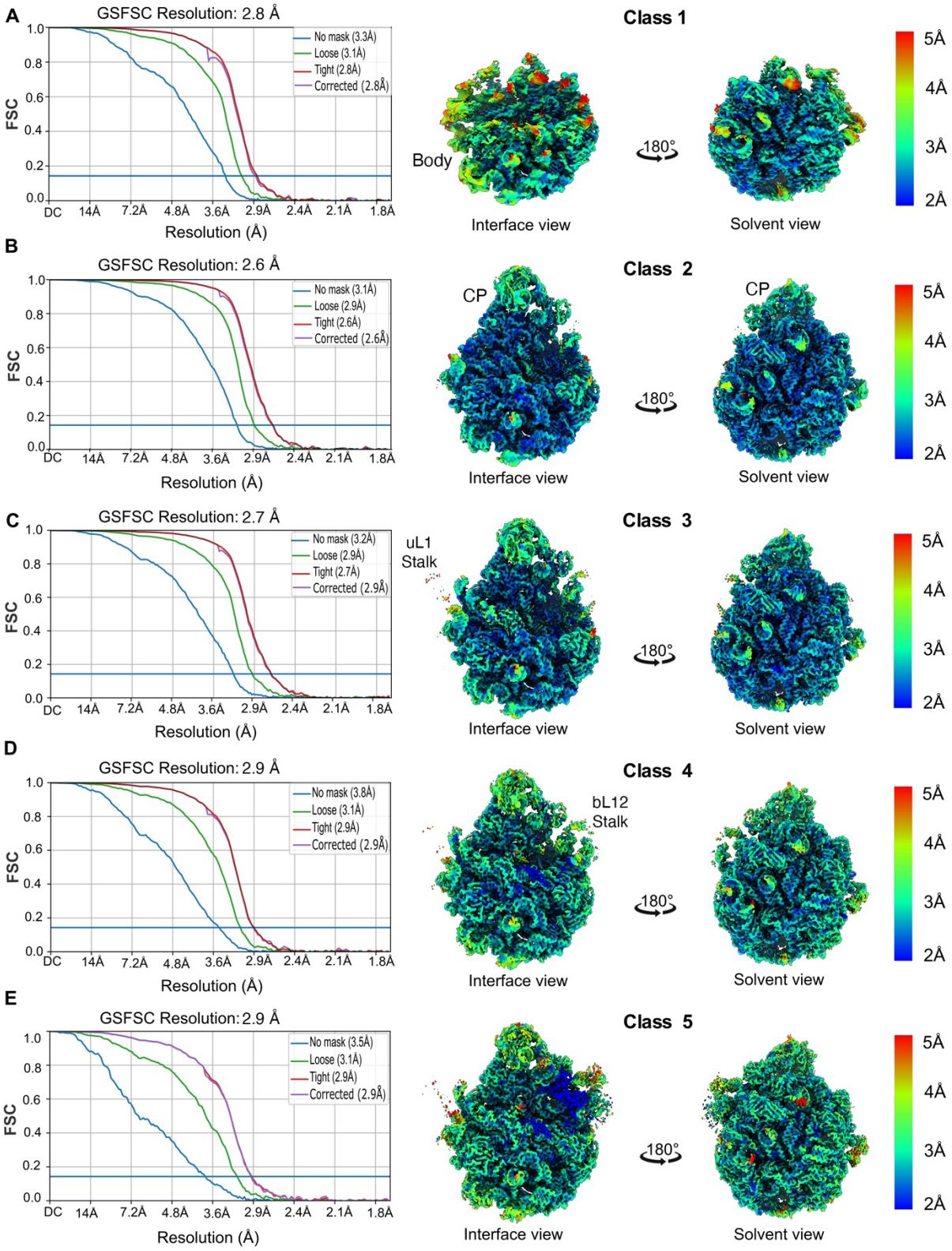
A
GSFSC Resolution: 2.8 Å
No mask (3.3Å)
Loose (3.1Å)
Tight (2.8Å)
Corrected (2.8Å)
FSC
Resolution (Å)
Class 1
Body
Interface view
180°
Solvent view
5Å
4Å
3Å
2Å
B
GSFSC Resolution: 2.6 Å
No mask (3.1Å)
Loose (2.9Å)
Tight (2.6Å)
Corrected (2.6Å)
Class 2
CP
C
GSFSC Resolution: 2.7 Å
No mask (3.2Å)
Loose (2.9Å)
Tight (2.7Å)
Corrected (2.9Å)
Class 3
uL1
Stalk
D
GSFSC Resolution: 2.9 Å
No mask (3.8Å)
Loose (3.1Å)
Tight (2.9Å)
Corrected (2.9Å)
Class 4
bL12
Stalk
E
GSFSC Resolution: 2.9 Å
No mask (3.5Å)
Loose (3.1Å)
Tight (2.9Å)
Corrected (2.9Å)
Class 5
DC
14Å
7.2Å
4.8Å
3.6Å
2.9Å
2.4Å
2.1Å
1.8Å

Supplementary Figure S3. ***Resolution analysis of the cryo-EM maps for the ΔSRL particles isolated from cells.*** *(A-E) Gold-Standard Fourier shell correlation (GSFSC) plots (left) for the cryo-EM maps obtained for the five classes of ΔSRL particles isolated from cells. The FSC curves were calculated using different masks. In the 'No Mask' plot, the raw FSC curve was calculated between two independent half-maps without masking. Loose': FSC calculated after applying a loose soft solvent mask to both half maps. The loose mask is calculated by thresholding the density map at 50% of the maximum density value. The resulting volume is dilated to create a soft mask. Voxels in the mask within 25 Å of the thresholded region receive a mask value of 1.0. Voxels between 25 and 40 Å fall off with a soft cosine edge, and voxels outside 40 Å receive a value of 0.0. 'Tight' is similar to the 'Loose' mask, except that the dilation distances are 6 Å for the value 1.0 distance and 12 Å for the value 0.0 distance. 'Corrected' uses the 'Tight' mask corrected by noise substitution. In this case, the two half maps have their phases randomized beyond a certain resolution, then the tight mask is applied to both, and a FSC is calculated. This FSC is used along with the original FSC before phase randomization to compute the corrected FSC. This accounts for correlation effects induced by masking. The resolution at which phase randomization begins is the resolution at which the no-mask FSC drops below the FSC = 0.143 criterion. The reported resolution is based on a FSC threshold of 0.143. The right panels show the front ('crown view') and back views of the cryo-EM maps obtained for these classes colored according to their local resolution. Local resolution scale bar and structural landmarks of the 50S subunit are indicated. CP means 'central protuberance'.*

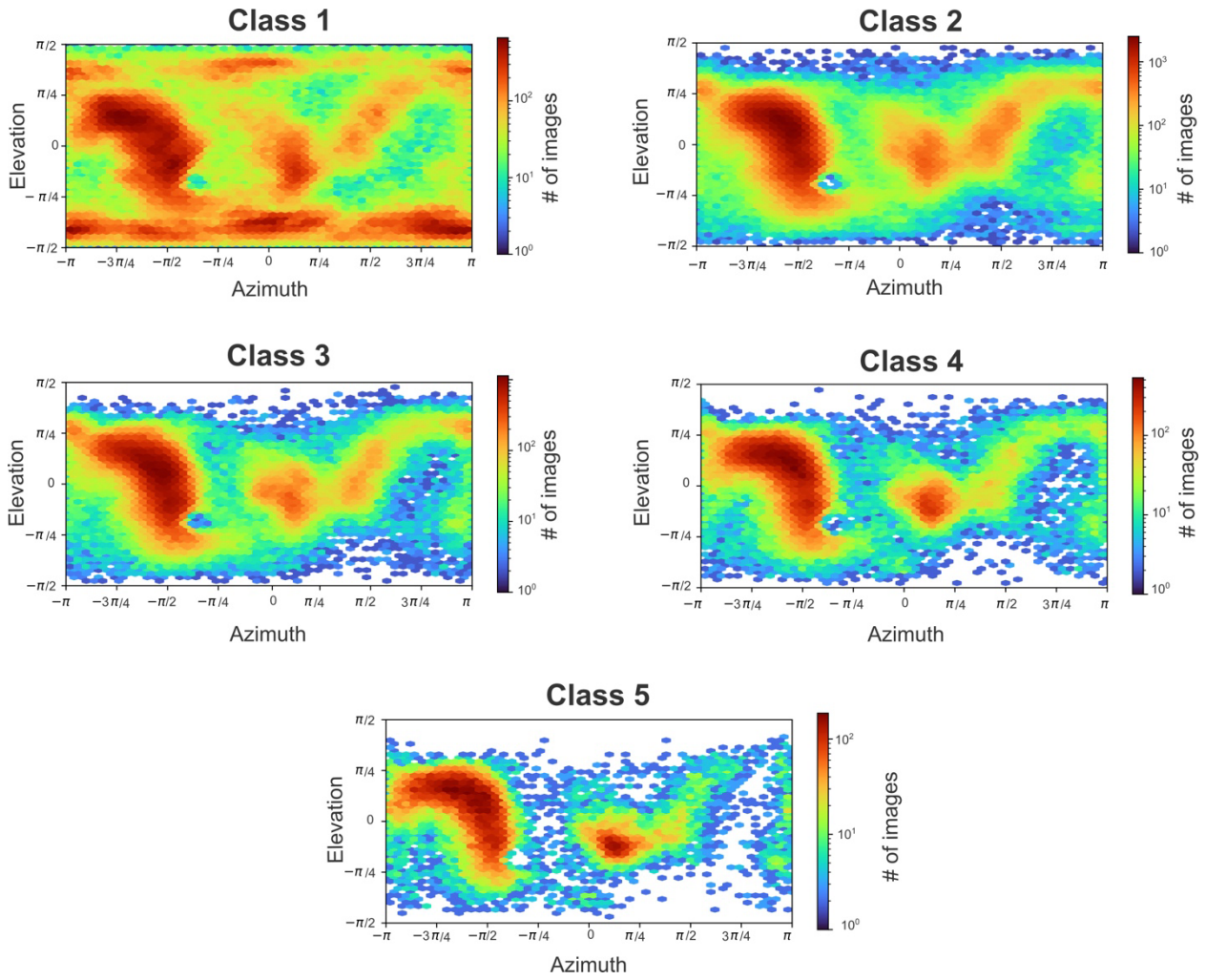

Supplementary Figure S4. ***Orientation distribution plots for each class obtained for the ΔSRL particles isolated from cells.*** *Plots showing the orientation distribution of the particles contributing to the Cryo-EM maps for each class. Each colored dot represents a single particle, and where multiple particles are oriented identically, the color changes according to the scale bar for each plot.*

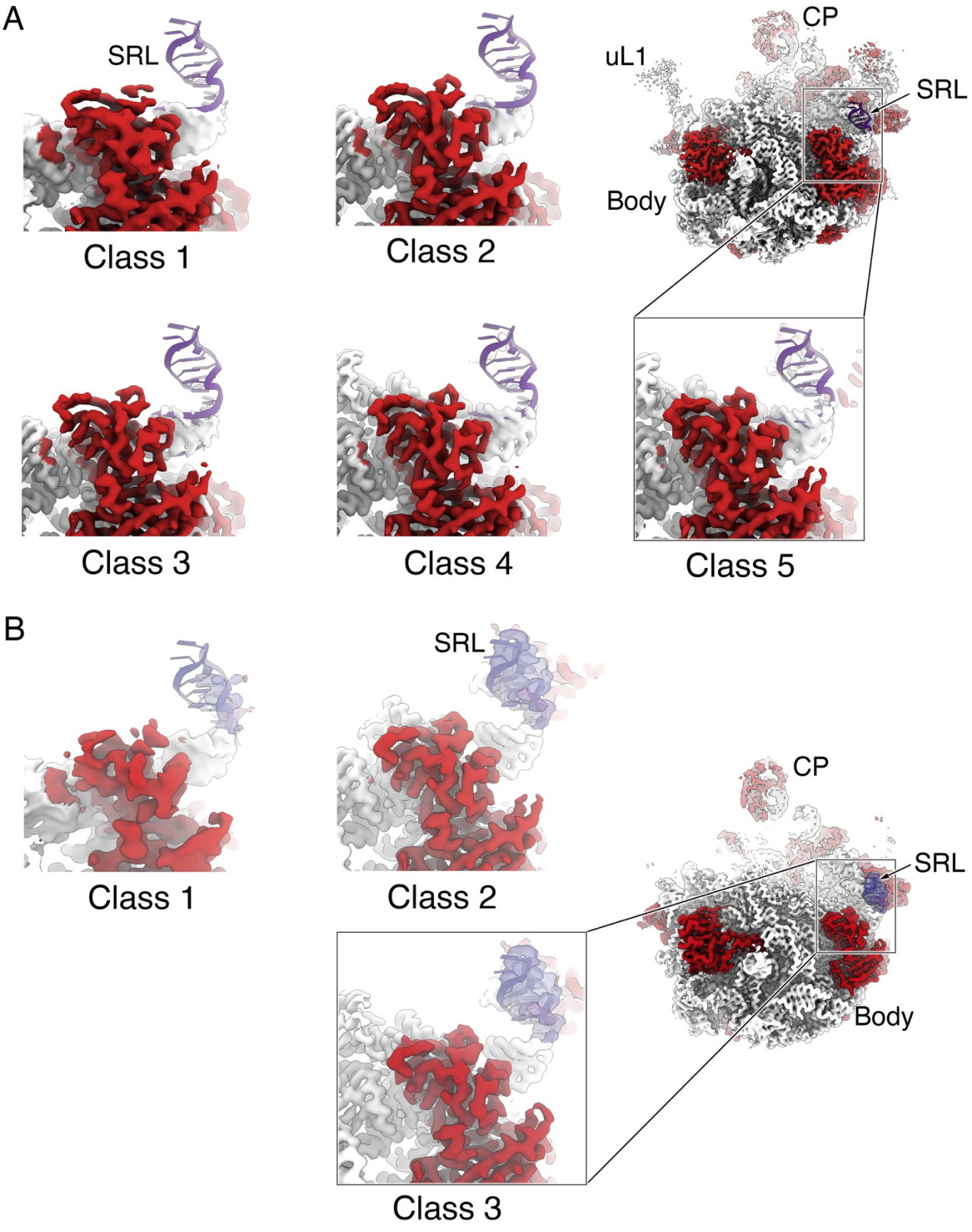
A
SRL
Class 1
Class 2
CP
uL1
SRL
Body
Class 3
Class 4
Class 5
B
Class 1
SRL
Class 2
CP
SRL
Body
Class 3

Supplementary Figure S5. ***The SRL motif in the cryo-EM maps.*** (A) *The area framed in the cryo-EM map obtained for class 5 of the ΔSRL particles isolated from cells (right top panel) is shown as a zoomed-in view in the panel below. The other zoomed-in views show the same area for the cryo-EM maps obtained for the other classes. None of these maps showed a density at the location of the SRL. The location of the SRL is indicated by the placement of the molecular model of this motif from PDB 4V4Q (Schuwirth et al. 2005). The rRNA is shown in light gray, and the r-proteins in dark red. The main landmarks of the 50S subunit are shown in the top right panel. CP stands for 'central protuberance'. (B) The panel was organized in a similar manner, showing the SRL in the three cryo-EM maps obtained for the particles isolated from wild-type cells. There is an apparent density for the SRL in the cryo-EM maps obtained for these classes. This density was only partial for the most immature class 1.*

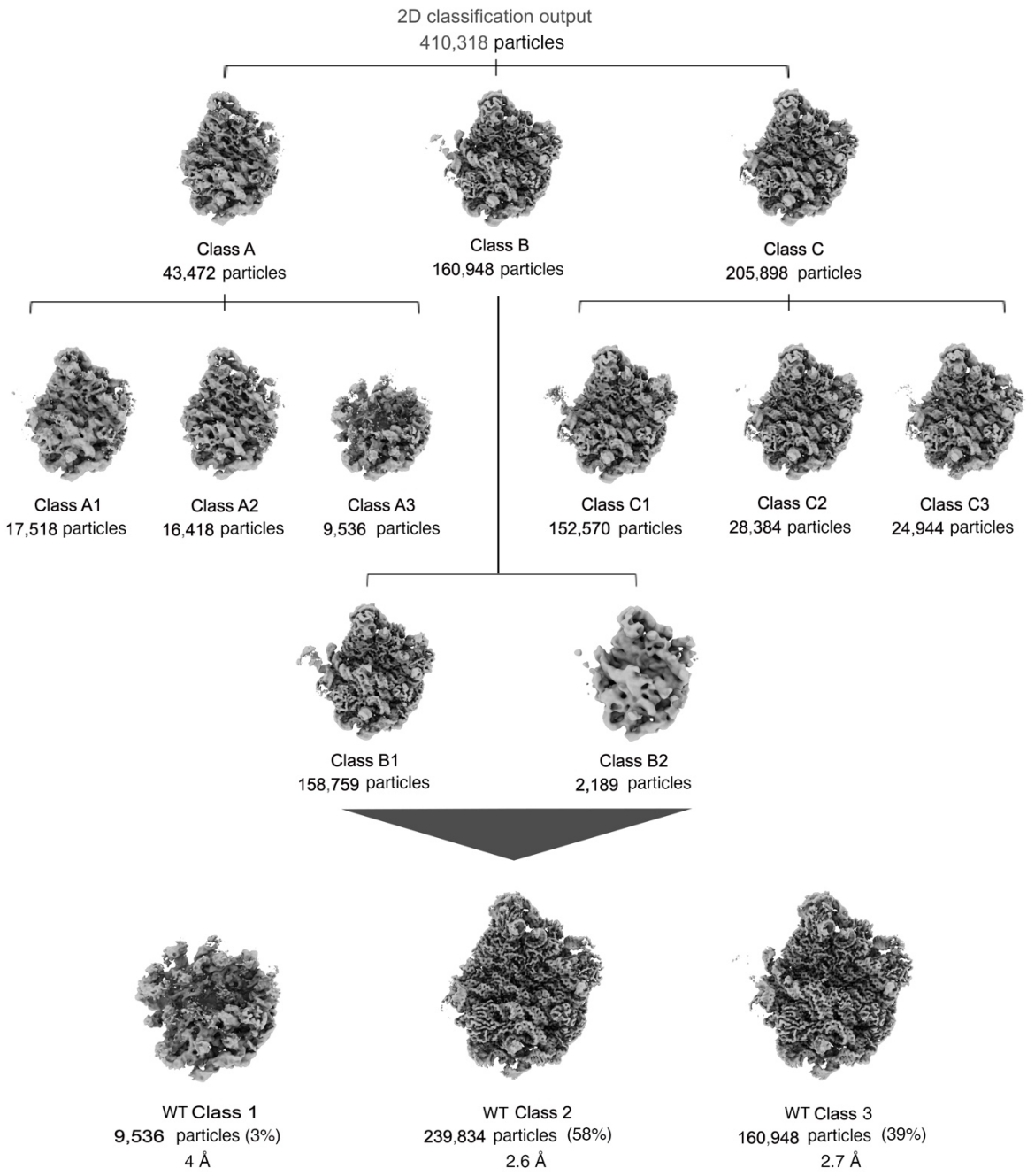

Supplementary Figure S6. ***3D classification and refinement workflow for the control particles isolated from cells.*** *Control particles isolated from cells were imaged by cryo-EM, and images were subjected to two layers of 3D classification. For each layer, particles were split into three or two new classes. The resulting subclasses were grouped into three main classes. Particles in each group were used to produce the high-resolution cryo-EM maps shown in Figure 3B. The high-resolution cryo-EM maps are shown unsharpened. The number of particles used for the final refinement of each class, the percentage of the total population they represent, and the obtained resolution are indicated.*

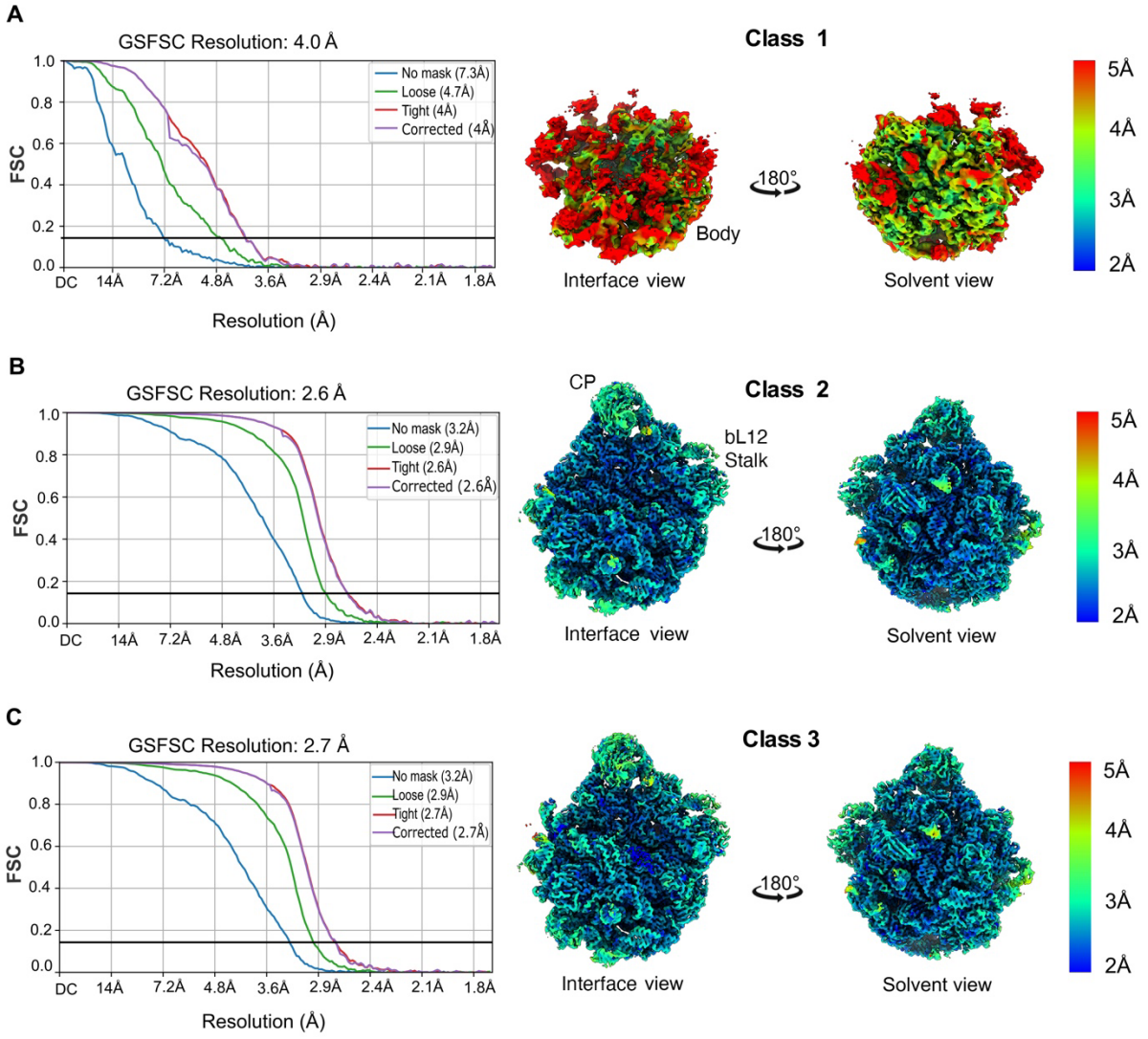

Supplementary Figure S7. ***Resolution analysis of the cryo-EM maps for the control particles isolated from cells.*** *(A-C) GSFSC plots (left) for the three classes of control particles isolated from cells. For each class, we show 'No mask', 'Loose', 'Tight', and 'Corrected' FSC curves calculated as described in the Supplementary Figure S2 legend. The reported resolution is based on a FSC threshold of 0.143. The right panels show the front ('crown view') and back views of the cryo-EM maps obtained for these classes colored according to their local resolution. Local resolution scale bar and structural landmarks of the 50S subunit are indicated. CP means 'central protuberance'.*

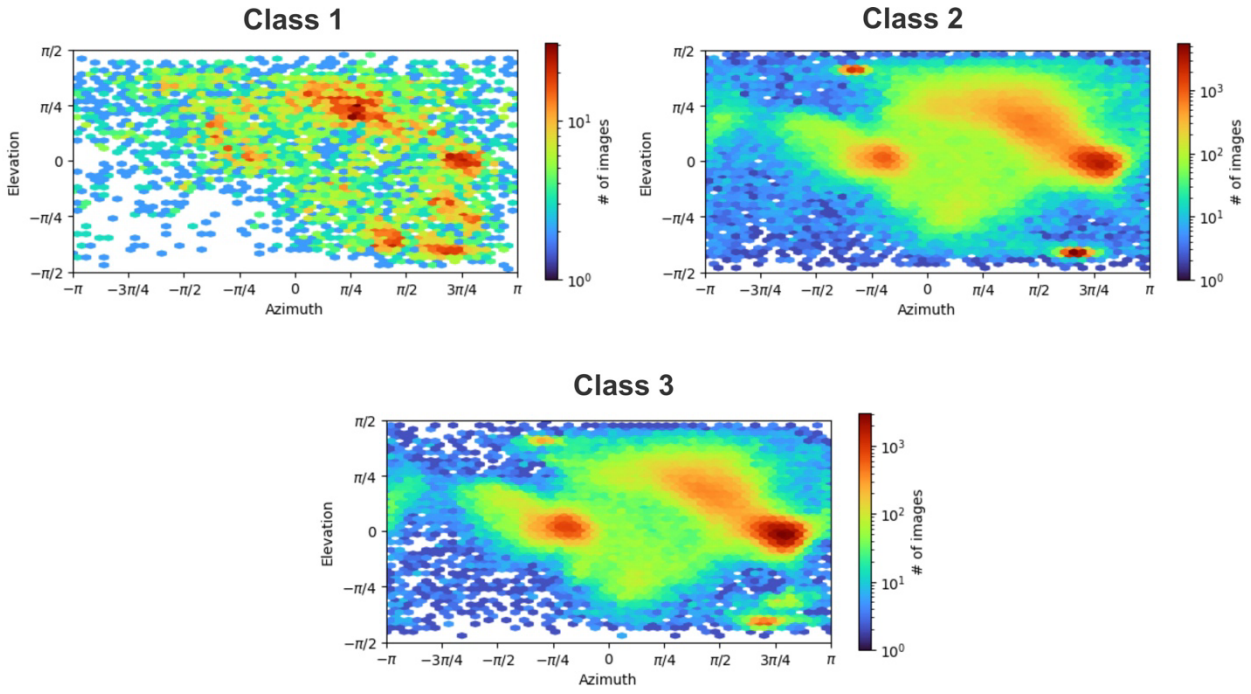

Supplementary Figure S8. ***Orientation distribution plots for each class of control particles isolated from cells.*** *Plots showing the orientation distribution of the particles contributing to the Cryo-EM maps for each class. Each colored dot represents a single particle, and where multiple particles are oriented identically, the color changes according to the scale bar for each plot.*

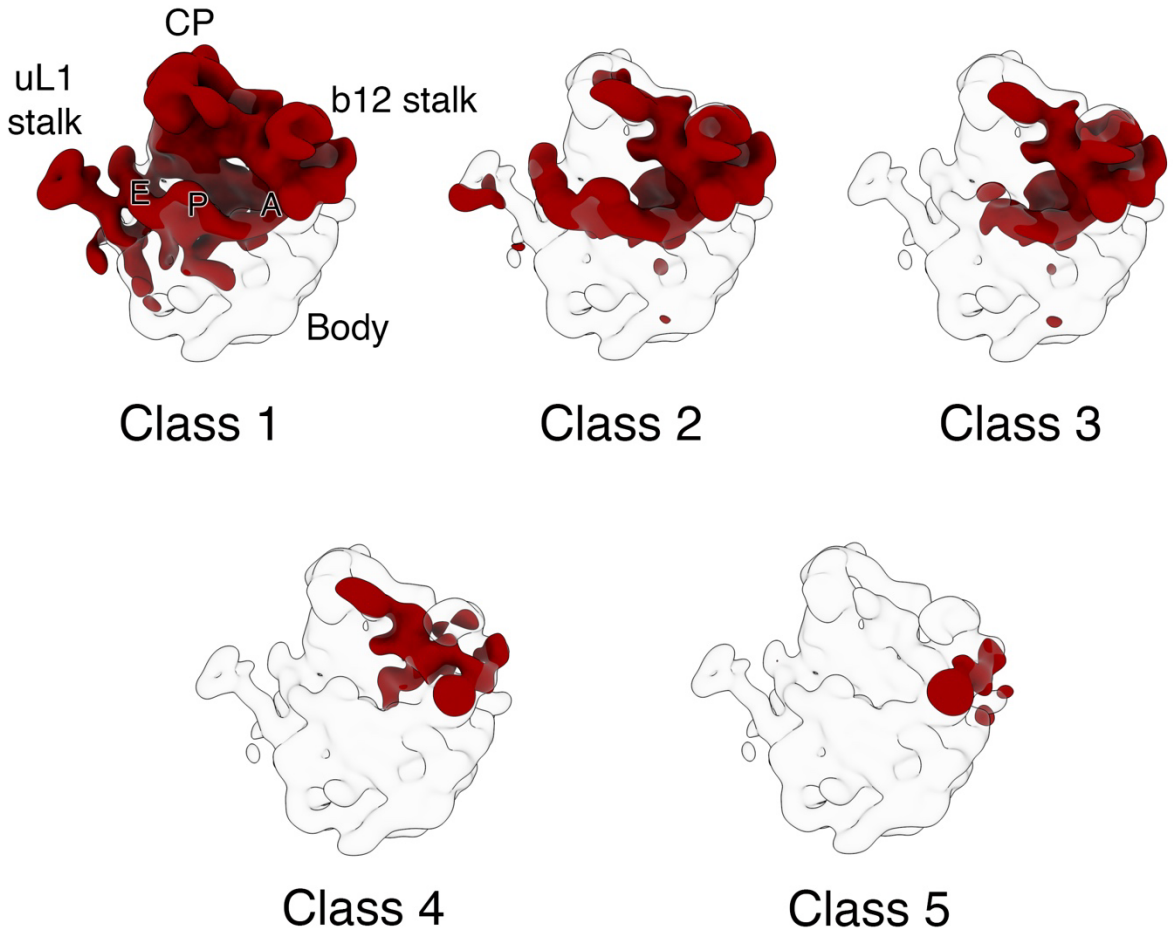

Supplementary Figure S9. ***Difference map analysis of the ΔSRL particles isolated from cells.*** *Difference maps obtained for the five classes of ΔSRL ribosomal particles isolated from cells. These maps were calculated by subtracting the map of each class from the cryo-EM map of the mature 50S subunit (control sample, class 3). To facilitate interpretation, the panels display the difference map for each class overlaid with a contour image of the mature 50S subunit. The main landmarks of the 50S subunit are labeled in the difference map for class 1. CP stands for central protuberance.*

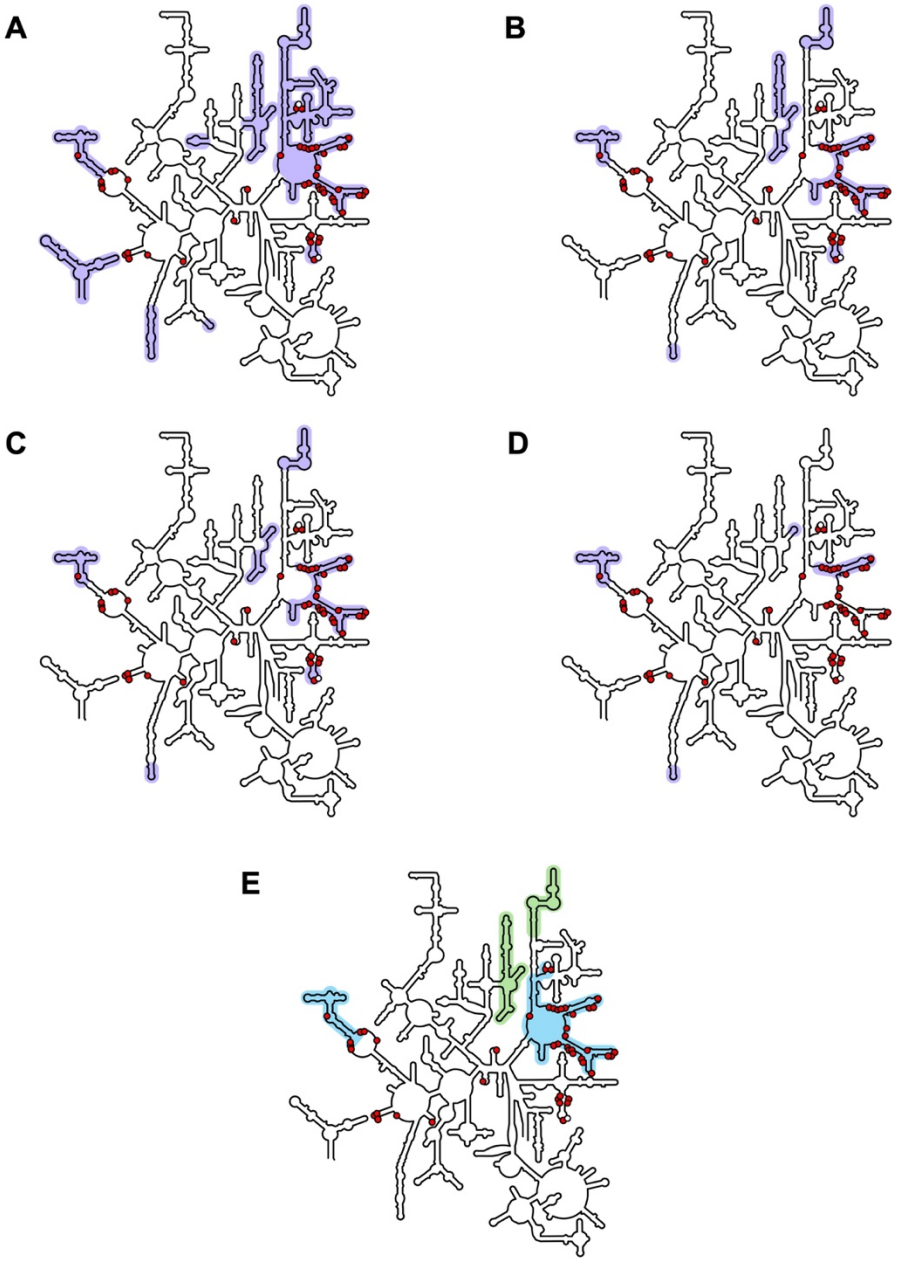

Supplementary Figure S10. ***Comparison of rRNA nucleotides of ΔSRL particles hyperreactive to chemical probes and disordered in cryo-EM maps.*** *Secondary structures of large subunit rRNA showing the disordered regions (purple highlight) in class 1 (A), class 2 (B), class 3 (C), and class 4 (D) maps of isolated ΔSRL particles. (E) Regions corresponding to block 4 (blue highlight) and block 5 (green highlight) (Davis et al. 2016). Red circles (A-E) indicate nucleotides hyperreactive to chemical probes (Lancaster et al. 2008).*

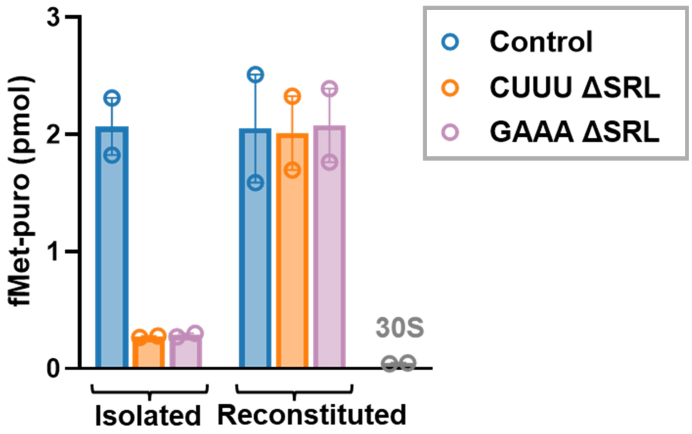

Supplementary Figure S11. ***Mutations that replace the SRL with either CUUU or GAAA confer indistinguishable effects.*** *Control or mutant particles (as indicated) were isolated from cells via affinity chromatography (isolated) or reconstituted in vitro (reconstituted) and assayed for peptidyl transferase activity. Gray symbols, 30S control.*

SUPPLEMENTARY TABLES

Supplementary Table S2. **Cryo-EM analysis of the ΔSRL particles isolated from cells:** Data acquisition parameters and map statistics.

Mutant ΔSRL particles isolated from cells					
Microscope	Titan Krios				
Detector	Gatan BioQuantum LS K3				
Nominal Magnification	105,000x				
Voltage (kV)	300				
Total exposure ($e^-/Å^2$)	40				
Number of frames	40				
Defocus range (μm)	-1.00 to -2.50				
Calibrated physical pixel size (Å/px)	0.855				
Reconstruction and refinement					
Classes	Class 1	Class 2	Class 3	Class 4	Class 5
Micrographs	13,036				
Particles	266,479	410,152	187,442	87,473	35,014
Resolution (Å)	2.8	2.6	2.7	2.9	2.9
Data Deposition					
EMDB code	EMDB- 47911	EMD-47913	EMD-47917	EMD-47918	EMD-47919

Supplementary Table S3. **Cryo-EM analysis of the control particles isolated from cells:** Data acquisition parameters and map statistics.

Control particles isolated from cells			
Microscope	Titan Krios		
Detector	Gatan BioQuantum LS K3		
Nominal Magnification	105,000x		
Voltage (kV)	300		
Total exposure ($e^-/Å^2$)	50		
Number of frames	30		
Defocus range (μm)	-1.00 to -2.50		
Calibrated physical pixel size (Å/px)	0.855		
Reconstruction and refinement			
Classes	Class 1	Class 2	Class 3
Micrographs	6,576		
Particles	9,536	239,834	160,948
Resolution (Å)	4	2.6	2.7
Data Deposition			
EMDB code	EMD-47920	EMD-47921	EMD-47922

SUPPLEMENTARY REFERENCES

Davis JH, Tan YZ, Carragher B, Potter CS, Lyumkis D, Williamson JR. 2016. Modular Assembly of the Bacterial Large Ribosomal Subunit. *Cell* **167**: 1610-1622 e1615.

Lancaster L, Lambert NJ, Maklan EJ, Horan LH, Noller HF. 2008. The sarcin-ricin loop of 23S rRNA is essential for assembly of the functional core of the 50S ribosomal subunit. *RNA* **14**: 1999-2012.

Schuwirth BS, Borovinskaya MA, Hau CW, Zhang W, Vila-Sanjurjo A, Holton JM, Cate JH. 2005. Structures of the bacterial ribosome at 3.5 A resolution. *Science* **310**: 827-834.